CONDUCTION AND CONVECTION HEAT TRANSFER CHARACTERISTICS OF WATER-BASED Au NANOFLUIDS IN A SQUARE CAVITY WITH DIFFERENTIALLY HEATED SIDE WALLS SUBJECTED TO CONSTANT TEMPERATURES

by

Primož TERNIK[a*] and Rebeka RUDOLF[b]

[a] Ternik Primož-Private researcher, Bresterniška ulica 163, 2354 Bresternica, Slovenia
[b] University of Maribor, Smetanova ulica 17, 2000 Maribor, Slovenia

Original Scientific Paper
DOI: 10.2298/TSCI130604082T

The present work deals with the natural convection in a square cavity filled with the water-based Au nanofluid. The cavity is heated on the vertical and cooled from the adjacent wall, while the other two horizontal walls are adiabatic. The governing differential equations have been solved by the standard finite volume method and the hydrodynamic and thermal fields were coupled together using the Boussinesq approximation. The main objective of this study is to investigate the influence of the nanoparticles' volume fraction on the heat transfer characteristics of Au nanofluids at the given base fluid's (i.e. water) Rayleigh number. Accurate results are presented over a wide range of the base fluid Rayleigh number and the volume fraction of Au nanoparticles. It is shown that adding nanoparticles in a base fluid delays the onset of convection. Contrary to many authors, it was shown here that the use of nanofluids can reduce the heat transfer rate instead of increasing it.

Key words: *Natural convection, Heat transfer, Nanofluid, Nusselt number*

Introduction

Today more than ever, ultrahigh-performance and controlled heat transfer plays an important role in the development of energy-efficient heat transfer systems and fluids which are required in many industries and commercial applications [1, 2]. The idea of improving the heat transfer performance of inherently poor conventional heat transfer fluids (e.g. water, oil or ethylene glycol) with the inclusion of solid particles was first introduced by Maxwell [3]. However, suspensions involving milli- or micro-sized particles create problems (such as sedimentation, clogging of channels, high pressure drop, and severe erosion of system boundaries) and cannot be used in microchannel flow passages. For that, nano-sized particles dispersed in a base fluid, known as nanofluid [4], have been developed, used and researched extensively to enhance heat transfer. Generally, the thermal conductivity of the particles, metallic or non-metallic, is typically an order of magnitude higher than that of the base fluids even at low concentrations resulting in an unquestionable heat transfer enhancement in forced convection applications [5-7]. But on the other hand, there is still a dispute on the role of nanoparticles on the heat transfer characteristics for the buoyancy driven flow. Natural convection (i.e. flow caused by the temperature induced density variations) is one of the most extensively analysed configurations because of its fundamental importance as the

* Corresponding author; e-mail: pternik@pt-rtd.eu

"benchmark" problem for studying convection effects (and comparing as well as validating numerical techniques). In addition to the obvious academic interest, this configuration has relevance in various engineering systems (e.g. compact heat exchangers [8] and cooling systems [9, 10], selective laser melting process [11]). Although quite some various different configurations of the enclosure problem are possible [12-18], one of the most studied cases involves the two-dimensional square enclosure with differentially heated isothermal vertical walls and adiabatic horizontal walls [19, 20]. When the vertical walls are insulated to ensure adiabatic conditions and the lower horizontal wall held at the higher temperature then one has the Rayleigh–Bénard configuration [21, 22].

The present study analyses the case where the horizontal walls are adiabatic and the temperature difference driving the convection comes from the sidewalls as in the classic benchmark paper of de Vahl Davis [23]. Although this configuration has been studied extensively for generalized Newtonian fluids, a comparatively limited effort has been directed towards the understanding of the natural convection of nanofluids. To date, most of the authors claim that the presence of nanoparticles in a fluid alters the flow structure and increases the natural convection heat transfer. Recent numerical studies by Ternik et al. [24], Ternik and Rudolf [25], Oztop et al. [26] and Abu-Nada and Oztop [27] illustrated that the suspended nanoparticles increase the heat transfer rate substantially for any given Rayleigh number. In addition they showed that the heat transfer rate in water-based nanofluids increases with an increasing volume fraction of Al_2O_3, Cu, TiO_2 and Au nanoparticles.

On the other hand, an apparently paradoxical behaviour of heat transfer deterioration was observed in experimental studies. For example, Putra et al. [28] reported that the presence of Al_2O_3 and CuO nanoparticles in a base fluid reduce the natural convective heat transfer for the natural convection inside a horizontal cylinder heated from one end and cooled from the other. However, they did not explain clearly why natural convective heat transfer is decreased with an increase in volume fraction of nanoparticles.

The above review of the existing literature shows that the problem of natural convection in a square enclosure filled with a water-based nanofluids is an issue still far from being solved completely. Framed in this general background, the purpose of the present study is to examine the effect of adding Au nanoparticles to the base fluid (i.e water) on the conduction and convection heat transfer characteristics in a square cavity with differentially heated vertical and adiabatic horizontal walls over a wide range of the fluid's Rayleigh number and volume fraction. In the present work we show that the relation expressing the local Nusselt number which is still used by many authors [13, 26, 27] lead to results which differ significantly from the one obtained with the thermodynamically valid (i.e. classical) expression [20-23] used in natural convection flows of a single-phase fluids. In addition, our numerical results show that the experimental results obtained by Putra et al. [28] are not at all paradoxical and provide an explanation for their experimental result.

The rest of the paper is organised as follows. The necessary mathematical background and numerical details are presented in the coming section, which is followed by the grid refinement, numerical accuracy assessment and validation study. Following this analysis, the results are presented and subsequently discussed. The main findings are summarised and conclusions are drawn in the final section of this paper.

Numerical method

The standard finite volume method, used successfully in many studies [19, 21, 24, 25, 29, 30], is used to solve the coupled conservation equations of mass, momentum and energy. In this framework, a second-order central differencing scheme is used for the diffusive terms and a second-order upwind scheme for the convective terms. Coupling of the pressure and velocity is achieved using the well-known SIMPLE (Semi-Implicit Method for Pressure-Linked Equations) algorithm [31]. The convergence criteria were set to 10^{-8} for all the relative (scaled) residuals.

Governing equations

For the present study, a steady-state flow of an incompressible water-based Au nanofluid is considered. It is assumed that both the fluid phase and nano-particles are in thermal and chemical equilibrium. Except for the density, properties of nanoparticles and fluid are taken to be constant. Table 1 presents the thermo-physical properties of water and gold at the reference temperature. It is also assumed that the Boussinesq approximation is valid for the buoyancy force. Governing equations (mass, momentum and energy conservation) of such a flow are [24-27]:

$$\frac{\partial v_i}{\partial x_i} = 0 \tag{1}$$

$$\rho_{nf} v_j \frac{\partial v_i}{\partial x_j} - \frac{\partial}{\partial x_j}\left(\eta_{nf} \frac{\partial v_i}{\partial x_j}\right) = -\frac{\partial p}{\partial x_i} + (\rho\beta)_{nf}\, g\left(T - T_C\right) + \frac{\partial}{\partial x_j}\left(\eta_{nf} \frac{\partial v_j}{\partial x_i}\right) \tag{2}$$

$$\left(\rho c_p\right)_{nf} v_j \frac{\partial T}{\partial x_j} = \frac{\partial}{\partial x_j}\left(k_{nf} \frac{\partial T}{\partial x_j}\right) \tag{3}$$

where the cold wall temperature T_C is taken to be the reference temperature for evaluating the buoyancy term in the momentum conservation equation.

Table 1. Thermo-physical properties of the water-based Au nanofluid [21, 24, 25].

	$\eta\left[Pas\right]$	$\rho\left[kgm^{-3}\right]$	$c_p\left[Jkg^{-1}K^{-1}\right]$	$k\left[Wm^{-1}K^{-1}\right]$	$\beta\left[K^{-1}\right]$
Pure water	$1.003\cdot10^{-3}$	997.1	4179	0.613	$2.1\cdot10^{-4}$
Au	/	19320	128.8	314.4	$1.416\cdot10^{-7}$

Relationships between the properties of nanofluid (nf) to those of base fluid (bf) and pure solid (s) are given with the following empirical models [24-27]:

- Density: $\rho_{nf} = (1-\varphi)\rho_{bf} + \varphi\rho_s$
- Dynamic viscosity: $\eta_{nf} = \eta_{bf} / (1-\varphi)^{2.5}$
- Thermal expansion: $(\rho\beta)_{nf} = (1-\varphi)(\rho\beta)_{bf} + \varphi(\rho\beta)_s$
- Heat capacitance: $\left(\rho c_p\right)_{nf} = (1-\varphi)\left(\rho c_p\right)_{bf} + \varphi\left(\rho c_p\right)_s$
- Thermal conductivity: $k_{nf} = k_{bf} \dfrac{k_s + 2k_{bf} - 2\varphi\left(k_{bf} - k_s\right)}{k_s + 2k_{bf} + \varphi\left(k_{bf} - k_s\right)}$

Geometry and boundary conditions

The simulation domain is shown schematically in fig. 1, where the two vertical walls of a square cavity are maintained at different and constant temperatures ($T_H > T_C$), whereas the other boundaries are considered to be adiabatic in nature. Both velocity components (i.e. v_x and v_y) are identically zero on each boundary because of the no-slip condition and impenetrability of rigid boundaries. The adiabatic temperature boundary conditions for the horizontal insulated boundaries are given by $\partial T/\partial y = 0$ at $y = 0$ and $y = L$.

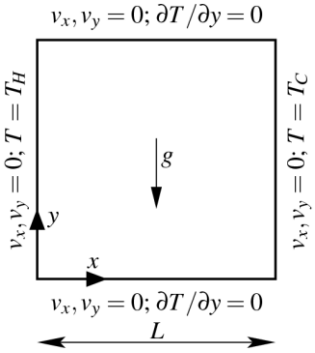

Figure 1. Schematic diagram of the simulation domain.

To study the heat-transfer characteristics due to the natural convection in nanofluids we introduced the local Nusselt number defined as [20-23]:

$$Nu = \frac{Q_{nf,conv}}{Q_{nf,cond}} = \frac{h_{nf} L}{k_{nf}} = -\frac{L}{T_H - T_C} \left.\frac{\partial T}{\partial x}\right|_{x=0} \tag{4}$$

where Nu presents the ratio of heat transfer rate by convection to that by conduction in the nanofluid in question, k_{nf} is the thermal conductivity and h_{nf} is the convection heat transfer coefficient of the nanofluid:

$$h_{nf} = -k_{nf} \left.\frac{\partial T}{\partial x}\right|_{x=0} \frac{1}{T_H - T_C} \tag{5}$$

It should be noted that the local Nusselt number as defined by eq. (4) differs from the form that is still used frequently for the nanofluids, e.g [13, 26, 27]:

$$Nu^* = \frac{Q_{nf,conv}}{Q_{bf,cond}} = -\frac{L}{T_H - T_C} \frac{k_{nf}}{k_{bf}} \left.\frac{\partial T}{\partial x}\right|_{x=0} \tag{6}$$

However, we believe that this definition of Nu^* is inappropriate (from the thermo-dynamic point of view), because its value is always greater than 1.0 for $\varphi > 0\%$ and this, in turn, means, that the heat transfer in nanofluids cannot take place solely by the thermal conduction.

Finally, in the present numerical study, the heat transfer characteristics are analysed in terms of the mean Nusselt number [19-27]:

$$\overline{Nu} = \frac{1}{L}\int_{y=0}^{y=L} Nu(y)dy \tag{7}$$

and the ratio of the nanofluid heat transfer rate to the base fluid one [21]:

$$\frac{Q_{nf}}{Q_{bf}} = \frac{k_{nf}\,\overline{Nu}_{nf}}{k_{bf}\,\overline{Nu}_{bf}} \tag{8}$$

at the same value of the base fluid Rayleigh number.

In order to investigate the influence of volume fraction on the heat transfer characteristics, the Rayleigh and the Prandtl number of the nanofluid can be expressed as [21]:

$$Ra_{nf} = \frac{(\rho\beta)_{nf}}{(\rho\beta)_{bf}}\frac{k_{bf}}{k_{nf}}\frac{(\rho c_p)_{nf}}{(\rho c_p)_{bf}}\frac{\eta_{bf}}{\eta_{nf}}Ra_{bf} \quad Pr_{nf} = \frac{\eta_{nf}}{\eta_{bf}}\frac{c_{p,nf}}{c_{p,bf}}\frac{k_{bf}}{k_{nf}}Pr_{bf} \tag{8}$$

Using eq. (8) we show that $Ra_{nf} < Ra_{bf}$ and $Pr_{nf} < Pr_{bf}$ for all values of φ for the nanofluids (fig. 2). The ratio of the nanofluid Rayleigh number to the base fluid Rayleigh number and nanofluid Prandtl number to the base fluid Prandtl number decreases with the volume fraction of nanoparticles; i.e. for a fixed value of Ra_{bf} and Pr_{bf}, the value of Ra_{nf} and Pr_{nf} decreases when adding nanoparticles.

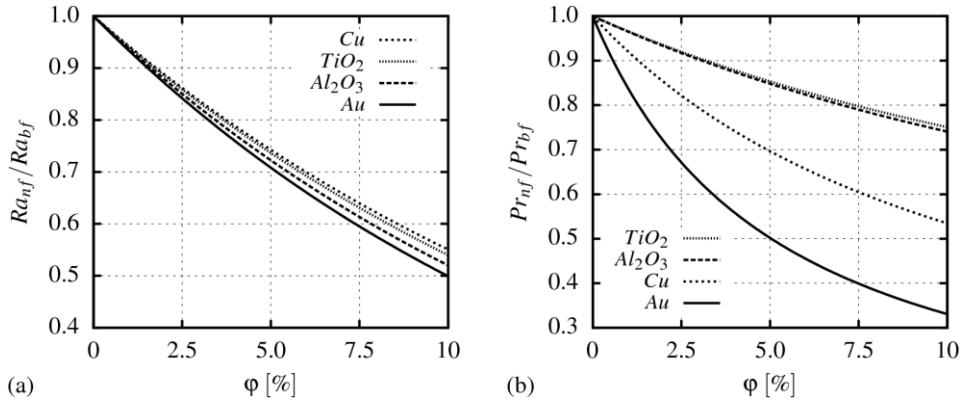

Figure 2. Variation of Rayleigh number (a) and Prandtl number (b) of various nanofluids.

Grid refinement, numerical accuracy and validation

The grid independence of the present results has been established on the basis of a detailed analysis at $Ra_{bf}=10^5$ and $\varphi = 10\%$ using three different non-uniform meshes (elements were concentrated towards each solid wall), the details of which are presented in tab. 2. The table includes number of elements in a particular direction, as well as the normalized minimum cell size.

With each grid refinement the number of elements in a particular direction is doubled and the minimum element size is halved. Such a procedure is useful for applying the

Richardson's extrapolation technique, which is a method for obtaining a higher-order estimate of the flow value (value at infinite grid) from a series of lower-order discrete values [32, 33].

Table 2. Characteristics of numerical meshes.

	Mesh M1	Mesh M2	Mesh M3
$N_x \times N_y$	50×50	100×100	200×200
$\Delta_{\min}/L$	$2.0000\cdot 10^{-3}$	$1.0000\cdot 10^{-3}$	$5.0000\cdot 10^{-4}$

For the general primitive variable ϕ the grid-converged (i.e., extrapolated to the zero element size) value according to Richardson extrapolation is given by $\phi_{ext} = \phi_{M3} - \left(\phi_{M2} - \phi_{M3}\right) \Big/ \left(r^p - 1\right)$ where ϕ_{M3} is obtained on the basis of the finest grid and ϕ_{M2} solution based on the next level of the coarse grid, $r = 2$ is the ratio between the coarse- and the fine-grid spacing and $p = 2$ is the expected order of accuracy.

The "percent numerical error" $Error = \left|\left(\phi_{M2} - \phi_{ext}\right)/\phi_{ext}\right| \cdot 100\%$ for the mean Nusselt number and the maximum non-dimensional vertical velocity component are presented in tab. 3. It can be seen that the differences in the grid refinements are exceedingly small and the agreement between mesh M2 and the extrapolated value is extremely good (the discretisation error levels are smaller than 0.40 %). Based on this, the simulations in the remainder of the paper were conducted on Mesh M2 which provided a reasonable compromise between high accuracy and computational efficiency.

Table 3. Grid refinement and numerical accuracy study.

	Mesh M1	Mesh M2	Mesh M3	ϕ_{ext}	*Error*
$\overline{Nu}$	3.7800	3.7892	3.7915	3.7922	0.08%
$v^*_{y,\max}$	49.8354	50.3041	50.4433	50.4897	0.37%

In addition to the aforementioned grid-dependency study, the present numerical results have also been compared against the well-known benchmark data of De Vahl Davis [23] and recent results of Turan et al. [34] for natural convection of the Newtonian fluid in a square cavity for the Rayleigh number values ranging from 10^3 to 10^6.

Table 4. Comparison of present results for the mean Nusselt number with other authors.

	$Pr = 0.71$		$Pr = 7$	
	Present	[23]	Present	[34]
$Ra = 10^3$	1.117	1.118	1.117	1.118
$Ra = 10^4$	2.242	2.245	2.272	2.274
$Ra = 10^5$	4.517	4.520	4.719	4.722
$Ra = 10^6$	8.820	8.823	9.719	9.222

The comparisons (summarized in tab. 4) between the present simulation results for the mean Nusselt number with the corresponding benchmark values were found to be excellent and entirely consistent with the aforementioned grid-dependency analysis.

Results and discussion

Temperature and velocity flow field

It is useful to inspect the distributions of dimensionless temperature θ and dimensionless vertical velocity v_y^* in order to understand the influences of Ra_{bf} and φ on the heat transfer characteristics during natural convection of water-based Au nanofluid in a square enclosure. The distributions of θ and v_y^* along the horizontal mid-plane $y/L = 0.50$ are shown in fig. 3.

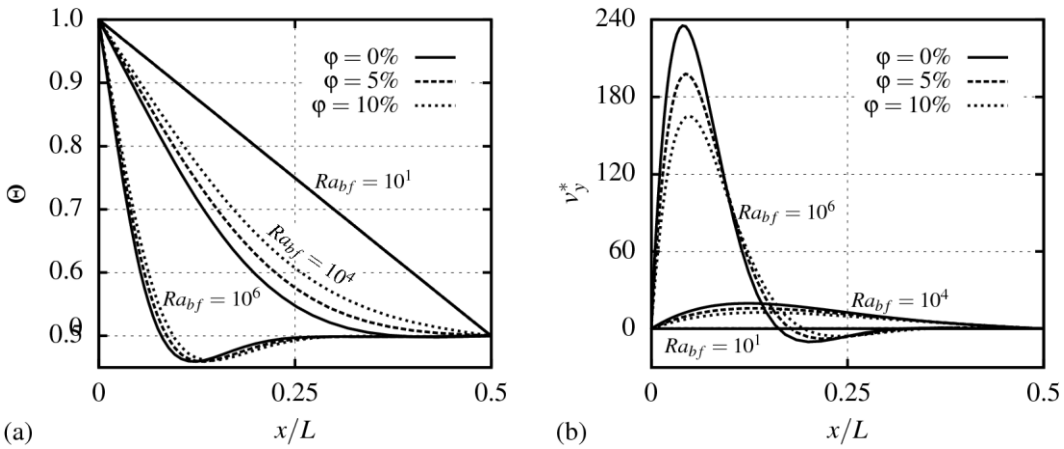

Figure 3. Variations of non-dimensional temperature (a) and non-dimensional vertical velocity component (b) along the horizontal mid-plane.

It is evident from fig. 3a that the distributions of θ become increasingly non-linear for increasing values of Ra_{bf}. This statement is supported by the data plotted in fig. 3b which demonstrates that the magnitude of the velocity component increases significantly with increasing Ra_{bf}. For a given set of values of φ an increase in Ra_{bf} gives rise to strengthening of buoyancy forces in comparison to viscous forces, which can be seen from fig. 3b, where the magnitude of v_y^* increases with increasing Ra_{bf}. As the convective transport strengthens with increasing Ra_{bf} the distribution of θ becomes significantly more non-linear with increasing Ra_{bf}, see fig. 3a.

At Ra_{bf}=10 the distribution of θ is completely linear and the vertical velocity component is essentially negligible due to very weak flow as the effects of buoyancy forces are dominated by viscous effects. Under this circumstance, the heat transfer takes place principally by conduction across the square enclosure. The effects of buoyancy force strengthen relative to the viscous force with increasing Ra_{bf}, which, in turn, augments heat transfer by convection due to stronger buoyancy-driven flow with higher vertical velocity magnitude. This effect is clearly evident from fig. 3, which indicates that the vertical velocity magnitude does indeed increase with increasing Ra_{bf} and that the distribution of non-dimensional tempe-

rature becomes increasingly non-linear with the strengthening of convective transport for higher values of Ra_{bf}.

On the other hand, fig. 3a illustrates that the thermal boundary layer thickness next to the heated wall is influenced by the addition of nanoparticles to the base fluid. This sensitivity of thermal boundary layer thickness to the volume fraction of nanoparticles is related to the increased thermal conductivity of the water-based Au nanofluid. As a matter of fact, increased values of the thermal conductivity are accompanied by the higher values of thermal diffusivity and the higher values of thermal diffusivity result in a reduction in the temperature gradients and, accordingly, increase the thermal boundary thickness as demonstrated in fig. 3a. Finally, this increase in the thermal boundary layer thickness reduces the Nusselt number values.

Mean Nusselt number

Figure 4 presents the variation of the mean Nusselt number along the heated wall with the Rayleigh number. For smaller values of the base- and nanofluid Rayleigh number there is no convection in the nanofluid or the base fluid, and the heat transfer occurs due to pure conduction, so the mean Nusselt number equals 1.0 and its value is independent of the Rayleigh number. As the base fluid Rayleigh number increases, the nanofluid remains in the conductive regime, while convection appears in the base fluid.

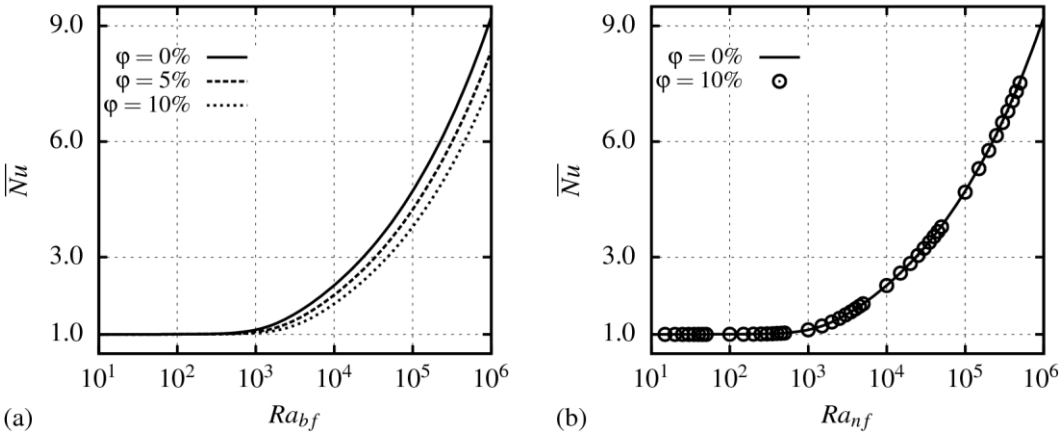

Figure 4. Variation of the mean Nusselt number with the base fluid Rayleigh number (a) and the nanofluid Rayleigh number (b).

The point of occurrence of the convective heat transfer regime (i.e. the critical value of the base fluid Rayleigh number at which the mean Nusselt number equals 1.01) depends on the volume fraction of Au nanoparticles. The higher is the value of volume fraction, the more delayed is the onset of convection (fig. 5a). When the nanofluid is in the convective heat-transfer regime, the mean Nusselt number is a monotonic increasing function of the Rayleigh number (figs. 4 and 5) and attains lower values for higher nanoparticles' volume fraction (fig. 4) at a given base fluid Rayleigh number.

On the other hand, it is interesting to notice that the onset of convection occurs at the same critical value of the nanofluid Rayleigh number, i.e. $Ra_{nf,cr} \cong 264.6$ (fig. 5b). Moreover, the value of the mean Nusselt number at a given nanofluid Rayleigh number is prac-

tically independent of the nanoparticles' volume fraction (fig. 4b) which is consistent with the earlier findings in the context of the natural convection of generalized Newtonian fluids [22] as well as Au nanofluids [19, 21]. This finding is a reflection of the nanofluid Prandtl number values considered in the present study. Its value varies (decreases with the increasing volume fraction as shown in fig. 2b) from $Pr_{nf}(\varphi = 0\%) = 6.84$ to $Pr_{nf}(\varphi = 10\%) = 2.26$ and for this range of the nanofluid Prandtl number values (i.e. $Pr_{nf} > 1$) the hydrodynamic boundary layer thickness remains much greater than the thermal boundary layer thickness, and thus the transport characteristics are driven primarily by buoyancy and viscous forces, which is reflected in the weak Prandtl number dependence of the mean Nusselt number.

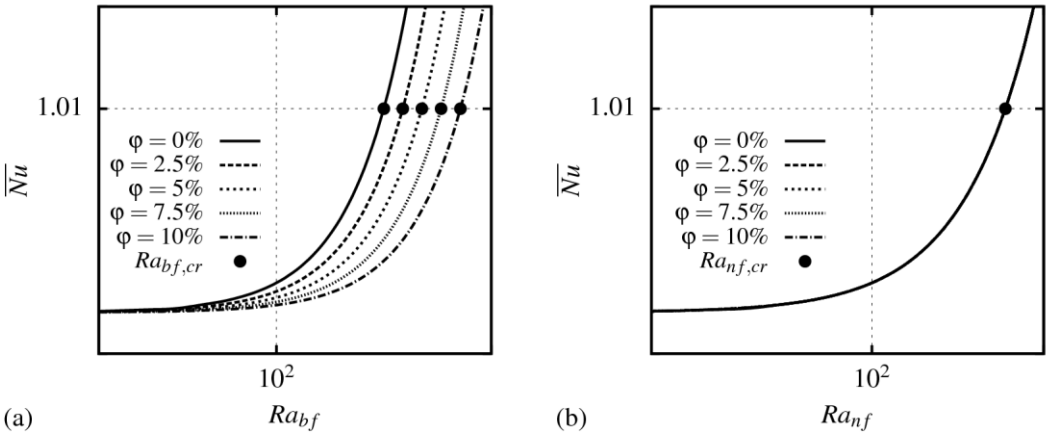

Figure 5. Onset of the heat transfer convection with the base fluid Rayleigh number (a) and the nanofluid Rayleigh number (b).

Heat transfer rate

Fig. 6a shows the effect of the base fluid Rayleigh number on the ratio of heat transfer rate for water-based Au nanofluid for different values of the volume fraction. In the range $Ra_{bf} < 264.6$ the heat transfer occurs by pure conduction, so the ratio of heat transfer is equal to the ratio of thermal conductivities and is constant and independent of the base fluid Rayleigh number. For $Ra_{nf} < 264.6$ and $Ra_{bf} > 264.6$ the nanofluid remains in the conductive regime, while convection appears in the base fluid. The heat transfer is more important in the base fluid than in the nanofluid and the ratio of the heat transfer rate is on a decrease. After the onset of the convective heat transfer regime in the nanofluid, the ratio of the heat transfer rate is on an increase but remains lower than the ratio that is obtained when both the nanofluid and the base fluid are in the conductive regime.

Finally, in fig. 6b, we observe that the heat transfer can decrease or increase depending on the value of the base-fluid Rayleigh number. It is true that the addition of Au nanoparticles in water increases its thermal conductivity, and, therefore improves the conductive heat transfer in the nanofluid compared to conductive heat transfer in the base fluid. But, on the other hand, just after the onset of convection adding nanoparticles enhances the heat transfer only for a given values of the temperature difference.

Last but not least, the present conclusions can be extrapolated to other water-based nanofluids (e.g. Cu, TiO_2 and Al_2O_3), since their nanofluid Rayleigh and Prandtl number values are within the range of the present (i.e. water-based Au nanoparticles) Rayleigh and Prandtl number values.

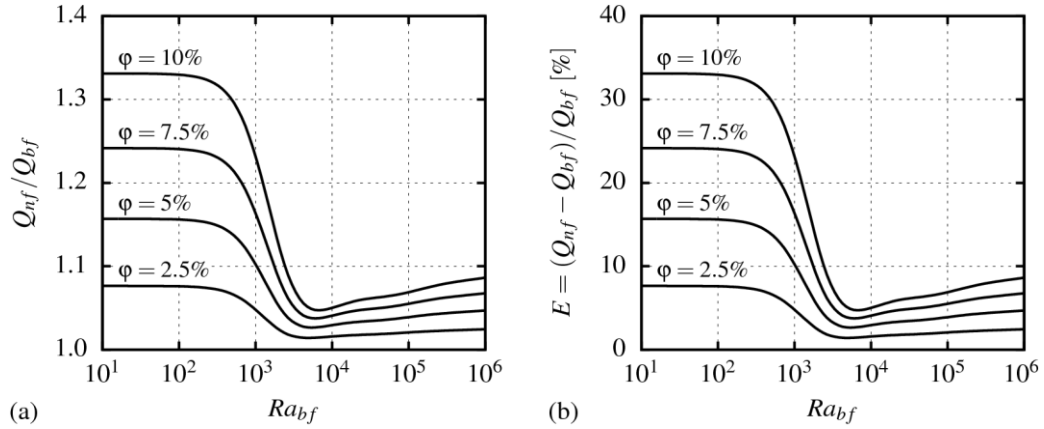

Figure 6. Effect of the base fluid Rayleigh number on the ratio (a) and the enhancement (b) of heat transfer rate.

Conclusions

In the present study, steady and laminar natural convection of water-based Au nanofluids in a square enclosure with differentially heated vertical walls have been studied by numerical means. The effects of the base- and nanofluid Rayleigh number and solid volume fraction on the heat and momentum transport characteristics have been investigated systematically.

The influence of computational grid refinement on the present numerical predictions was studied throughout the examination of grid convergence. By utilising extremely fine meshes the resulting discretisation error levels are below 0,40%.

The numerical method was validated for the case of Newtonian fluid natural convection in a square cavity for which the results are available in the open literature. Remarkable agreement of present results with the benchmark results yields sufficient confidence in the present numerical procedure and results.

Highly accurate numerical results pointed out some important points, such as:

- In the side heated square cavity configuration, just after the onset of convection, there is more heat transfer in the base fluid than in the nanofluid. For a fixed value of the base fluid Rayleigh number, the nanofluid Rayleigh number decreases with the increasing volume fraction of nanoparticles. Thus, the nanoparticles delay the onset of convection.
- The onset of the convective heat-transfer regime occurs at the same value of the nanofluid Rayleigh number.
- In the convective heat-transfer regime the mean Nusselt number increases monotonically with the base-fluid Rayleigh number, but the mean Nusselt number values obtained for the higher values of the nanoparticles' volume fraction are

smaller than those obtained in the case of the base fluid at with the same nominal values of the base fluid Rayleigh number.

- The values of the mean Nusselt number at a given nanofluid Rayleigh number are practically independent of the nanoparticles' volume fraction.
- The heat transfer rate can decrease or increase depending on the value of the base fluid Rayleigh number. So, an addition of nanoparticles increases the heat transfer only for the given values of the temperature difference.

Acknowledgement

The research leading to these results was carried out within the framework of the Research Project "Production technology of Au nano-particles" (L2-4212) and has received funding from the Slovenian Research Agency (ARRS).

References

[1] Neslusan, M.; Mrkvica, I., Cep, R., Kozak, D., Konderla, R., Deformations after heat treatment and their influence on cutting process, *Tech. Gaz.*, *18* (2011), 4, pp. 601-608
[2] Ghosh, A., Chattopadhyaya, S., Hloch, S., Prediction of weld bead parameters, transient temperature distribution & HAZ width of submerged arc welded structural steel plates, *Tech. Gaz.*, *19* (2012), 3, pp. 617-620
[3] Maxwell, J. C., *A Treatise on Electricity and Magnetism*, Clarendon Press, Oxford, UK, 1981
[4] Choi, S. U. S., Enhancing thermal conductivity of fluids with nanoparticles, *Dev. Appl. Non- Newtonian Flows*, *66* (1995), pp. 99-105
[5] Daungthongsuk, W., Wongwises, S., A critical review of convective heat transfer in nanofluids, *Renewable Sustainable Energy Rev.*, *11* (2007), 5, 797–817
[6] Rhi, S. H., Han, W. S., Thermal characteristics of grooved heat pipe with hybrid nanofluids, *Therm. Sci.*, *15* (2011), 1, pp. 195-206
[7] Fard, M. H., Talaie, M. R., Nasr, S., Numerical and experimental of heat transfer of ZnO/water nanofluid in the concentric tube and plate heat exchangers, *Therm. Sci.*, *15* (2011), 1, pp.183-194
[8] Rek, Z., Rudolf, M., Žun, Z., Application of CFD Simulation in the Development of a New Generation Heating Oven, *J. Mech. Eng.*, *58* (2012), 2, pp. 134-144
[9] Venko, S., Vidrih, B., Pavlovič, E., Medved, S., Enhanced Heat Transfer on Thermo Active Cooling Wall, *J. Mech. Eng.*, *58* (2012), 11, pp. 623-632
[10] Stritih, U., Butala, V., Energy Savings in Building with a PCM Free Cooling System, *J. Mech. Eng.*, *57* (2011), 2, pp. 125-134
[11] Contuzzi, N., Campanelli, S. L., Ludovico, A. D., 3D finite element analysis in the selective laser melting process, *Int. J. Simul. Model.*, *10* (2011), 3, pp. 113-121
[12] Mahmoudi, A. H., Shahi, M., Raouf, A. H., Modeling of conjugated heat transfer in a thick walled enclosure filled with nanofluid, *Int. Commun. Heat Mass Transfer*, *38* (2011), 1, pp. 119-127
[13] Saleh, H., Roslan, R., Hashim, I., Natural convection heat transfer in a nanofluid-filled trapezoidal enclosure, *Int. J. Heat Mass Transfer*, *54* (2011), 1-3, pp. 194-201
[14] Huelsz, G., Rechtman, R., Heat transfer due to natural convection in an inclined square cavity using the lattice Boltzmann equation method, *Int. J. Therm. Sci.*, *65* (2013), March, pp. 111-119
[15] Hasan, M. N., Saha, S. C., Gu, Y. T., Unsteady natural convection within a differentially heated enclosure of sinusoidal corrugated side walls, *Int. J. Heat Mass Transfer*, *55* (2012), 21-22, pp. 5696-5708
[16] Yesiloz, G., Aydin, O., Laminar natural convection in right-angled triangular enclosures heated and cooled on adjacent walls, *Int. J. Heat Mass Transfer*, *60* (2013), May, pp. 365-374
[17] Terekhov, V. I., Chichindaev, A. V., Ekaid, A. L., Buoyancy heat transfer in staggered dividing square enclosure, *Therm. Sci.*, *15* (2011), 2, pp.409-422
[18] Aich, W., Hajri, I., Omri, A., Numerical analysis of natural convection in a prismatic enclosure, *Therm. Sci.*, *15* (2011), 1, pp.437-446
[19] Ternik, P., Rudolf, R., Laminar natural convection of non-Newtonian nanofluids in a square enclosure with differentially heated side walls, *Int. J. Simul. Model.*, *12* (2013), 1, pp. 5-16

[20] Turan, O., Poole, R. J., Chakraborty, N., Influences of boundary conditions on laminar natural convection in rectangular enclosures with differentially heated side walls, *Int. J. Heat Fluid Flow, 33* (2012), 1, pp. 131-146
[21] Ternik, P., Rudolf, R., Žunič, Z., Numerical study of Rayleigh-Benard natural convection heat-transfer characteristics of water-based Au nanofluids, *Mater. Technol., 47* (2013), 2, pp. 211-215
[22] Turan, O., Chakraborty, N., Poole, R. J., Laminar Rayleigh Bénard convection of yield stress fluids in a square enclosure, *J. Non-Newtonian Fluid Mech., 171-172* (2012), 1, pp. 83-96
[23] De Vahl Davis, G., Natural convection of air in a square cavity: a benchmark numerical solution, *Int. J. Numer. Methods Fluids, 3* (1983), 3, pp. 249–264
[24] Ternik, P., Rudolf, R., Žunič, Z., Numerical study of heat transfer enhancement of homogeneous water-Au nanofluid under natural convection, *Mater. Technol., 46* (2012), 3, pp. 257-261
[25] Ternik, P., Rudolf, R., Heat transfer enhancement for natural convection flow of water-based nanofluids in a square enclosure, *Int. J. Simul. Model., 11* (2012), 1, pp. 29-39
[26] Oztop, H. F., Abu-Nada, E., Varol, Y., Al-Salem, K., Computational analysis of non-isothermal temperature distribution on natural convection in nanofluid filled enclosures, *Superlattices Microstruct., 49* (2011), 4, pp. 453-467
[27] Abu-Nada, E., Oztop, H. F., Effects of inclination angle on natural convection in enclosures filled with Cu–water nanofluid, *Int. J. Heat Fluid Flow, 30* (2009), 4, pp. 669-678
[28] Putra, N., Roetzel, W., Das, S. K., Natural convection of nano-fluids, *Heat Mass Transfer, 39* (2002), pp. 775-784
[29] Biluš, I., Ternik, P., Žunič, Z., Further contributions on the flow past a stationary and confined cylinder: Creeping and slowly moving flow of Power law fluids, *J. Fluids Struct., 27* (2011), 7, pp. 1278-1295
[30] Raić, K. T., Rudolf, R., Ternik, P., Žunič, Z., Lazić, V., Stamenković, D., Tanasković, T., Anžel, I., CFD analysis of exothermic reactions in Al-Au multi-layered foils, *Mater Technol., 45* (2011), 4, pp. 335-338
[31] Patankar, S. V., *Numerical Heat Transfer and Fluid Flow*, Hemisphere, Washington, USA, 1980
[32] Roache, P. J., Perspective: A method for uniform reporting of grid refinement studies, *J. Fluids Eng., 116* (1994), 3, pp. 405-413
[33] Ismail, C., Karatekin, O., Numerical experiments on application of Richardson extrapolation with non-uniform grids, *J. Fluids Eng., 119* (1997), 3, pp. 584-590
[34] Turan, O., Chakraborty, N., Poole, R. J., Laminar natural convection of Bingham fluids in a square enclosure with differentially heated side walls, *J. Non-Newtonian Fluid Mech., 165* (2010), 15-16, pp. 901-913

Paper submitted: June 4, 2013
Paper revised: June 5, 2013
Paper accepted: June 8, 2013